

A Comparison of the Mechanism for the Reductive Half-Reaction between Pea Seedling and Other Copper Amine Oxidases (CAOs)

RAJEEV PRABHAKAR, PER E. M. SIEGBAHN

Department of Physics, Stockholm Centre for Physics, Astronomy and Biotechnology (SC-FAB),
Stockholm University, S-106 91 Stockholm, Sweden

Received 1 November 2002; Accepted 12 February 2003

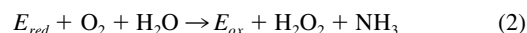
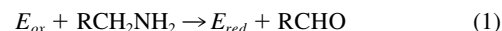
Abstract: In a previous DFT study a mechanism for the reductive half-reaction of pea seedling amine oxidase (PSAO) was suggested. In many of the suggested steps a lysine at the active site plays an important role. However, this lysine is not found in other amine oxidases. The primary aim of the present DFT study is therefore to investigate alternative mechanisms for those amine oxidases (CAO) where the lysine residue is not present. One of the most important roles suggested for the lysine in PSAO was to protonate the O2-site of TPQ before the critical C—H bond cleavage of the substrate. In the absence of lysine the O2-site of TPQ is now suggested to be protonated by a water ligand on the copper metal complex, in line with experimental suggestions. In other steps the role of lysine is taken over by an asparagine. All results are compared with experimental observations and good agreement is generally found.

© 2003 Wiley Periodicals, Inc. J Comput Chem 24: 1599–1609, 2003

Key words: transition states; density functional theory; mechanism; pea seedling amine oxidase (PSAO); copper amine oxidase (CAO)

Introduction

Copper containing amine oxidases (CAOs) constitute a family of redox active enzymes, which are present both in eukaryotes and prokaryotes. They catalyze the two-electron oxidative deamination of primary amines by dioxygen into corresponding aldehydes, ammonia, and hydrogen peroxide. In prokaryotes, amine oxidases are suggested to have nutrient associated functions,^{1–3} but in eukaryotes they are involved in a large variety of functions. They are implicated in lignification processes, wound healing, tissue differentiation, tumor growth, and programmed cell death.^{4–6} The CAO enzymes are homodimeric with 70–95 kDa subunits, and with each subunit containing one copper center and an organic cofactor 2,4,5-trihydroxyphenylalaninequinone referred to as topa quinone (TPQ).^{7–9} The crystal structures from *Escherichia coli* (ECAO),¹⁰ pea seedling (PSAO),¹¹ *Arthobacter globiformis* (APAO),¹² and yeast *Hansenula polymorpha* (HPAO)¹³ have been solved. Recently, Zn-substituted structures from the HPAO have been crystallized.¹⁴ CAOs are suggested to be dual-function enzymes, involved both in TPQ biogenesis from a precursor tyrosine^{15,16} and catalytic oxidative deamination of amines. Steady-state kinetics for the CAOs with regard to amine substrate and dioxygen has shown that the catalytic mechanism proceeds via two half-reactions known as the reductive and oxidative half-reactions,^{4,17} shown in Eqs. (1) and (2), respectively:



In the absence of dioxygen, kinetic constants obtained for the reduction of the enzyme are in good agreement with the steady-state parameters for the reductive half-reaction.¹⁸

The catalytic mechanism for the reductive half-reaction of PSAO has recently been investigated by DFT methods.¹⁹ This study was strongly guided by experimental structural and spectroscopic information, and the suggested mechanism is summarized in Figure 2. This mechanism is divided into six steps where steps 2 and 3 were further subdivided into two steps. In step 1, the amine substrate attacks the C5 site of TPQ accompanied by a simultaneous protonation by Asp300. In step 2a, a proton is transferred from the substrate to the O5 hydroxyl group via an external water, followed by its abstraction by Asp300. In step 2b, a donation of a proton by Asp300 to the O5 hydroxyl group of TPQ leads to the formation of a substrate Schiff base accompanied by a release of a water molecule. This substrate Schiff base has been found in a crystal structure with an inhibitor²⁰ and by resonance Raman spectroscopy.²¹ In the third step, Lys296 is suggested to play one

Correspondence to: R. Prabhakar; e-mail: raj@physto.se

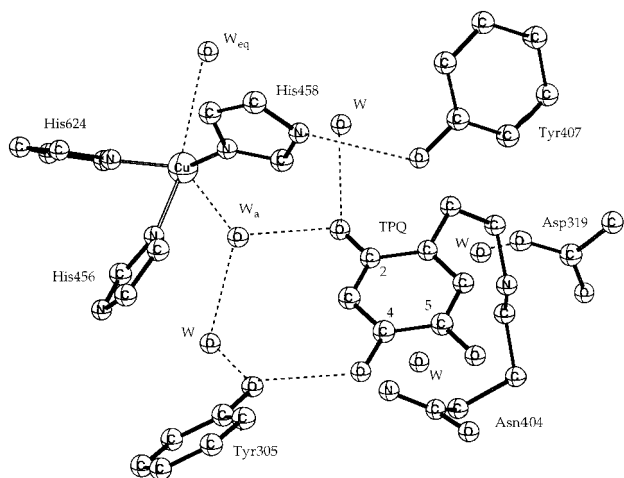


Figure 1. X-ray structure of the active site region of HPAO.

of its most important roles in the reductive half-reaction as the proton donor for the necessary protonation of the O2-site of TPQ. The protonation of O2 is important for the full utilization of the

resonance effects in the next critical C—H bond breaking step. According to the proposed mechanism, Lys296 uses a hydrogen bonded chain of two water molecules and Tyr286 to protonate the O2-site of TPQ. In step 3b, the C—H bond of the substrate is broken in a proton transfer step involving the deprotonated lysine, and a product Schiff base is formed. This step is found to be rate-limiting for the reductive half-reaction in agreement with experiments.²² The formation of this product Schiff base has been observed experimentally by resonance Raman spectroscopy for an E406N mutant of yeast methylamine oxidase.^{23,24} In step 4, Asp300 abstracts a proton from a solvent water and the activated hydroxyl group, in turn, attacks C1 of the substrate forming a C—OH bond. In step 5, Asp300 transfers its proton to the substrate N1 group through a hydrogen bonded chain involving a water molecule. In step 6, Asp300 plays the role of proton abstractor in the C—N bond cleavage and the product aldehyde is released. In this suggested mechanism for the reductive half-reaction of PSAO,¹⁹ it is clear that the lysine residue plays a quite important role. It is also known from experiments that the lysine residue is conserved only in approximately half of the known amine oxidase.²⁵ For example, as seen from the crystal structure of HPAO, the lysine is not present at the active site of this enzyme.¹³ This

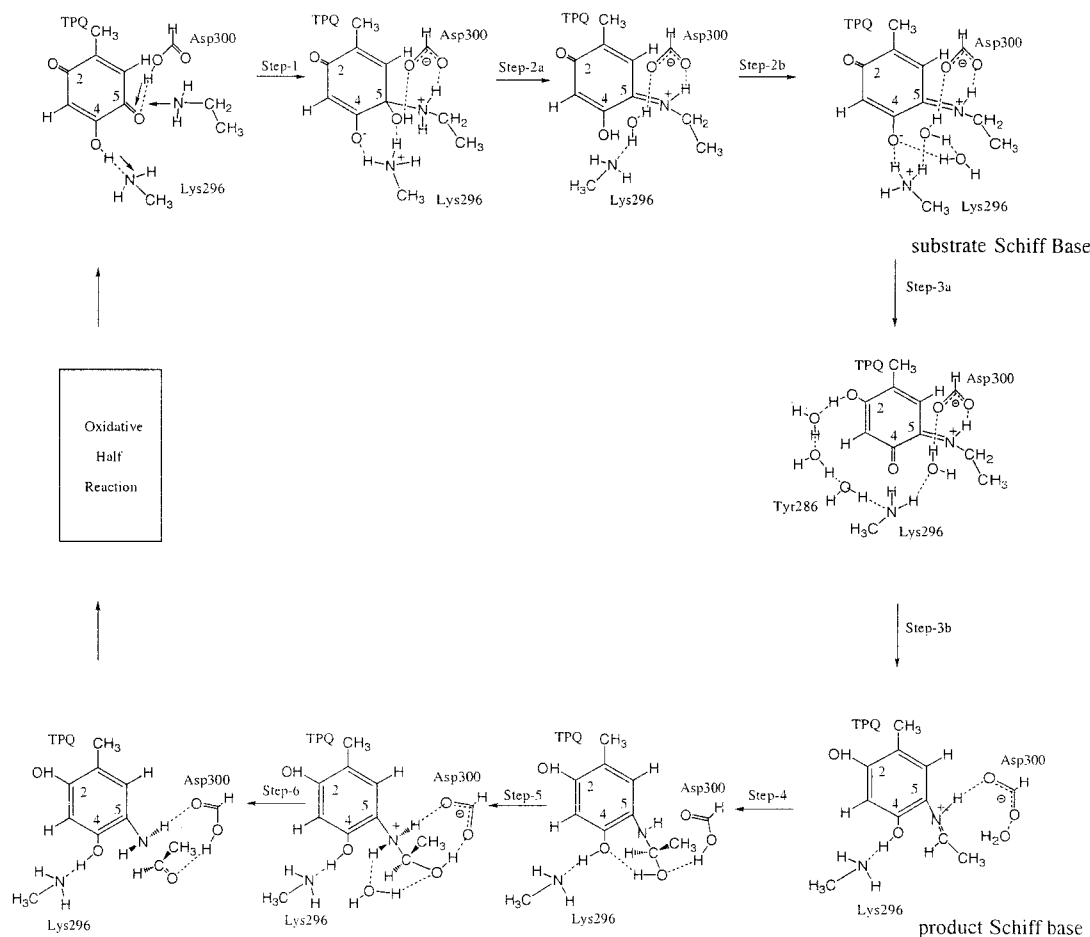


Figure 2. Theoretically suggested mechanism for the reductive half-reaction of PSAO.

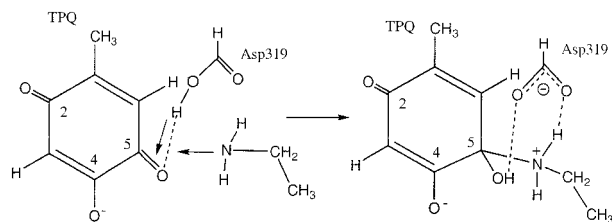


Figure 3. Suggested first step of the amine oxidation in HPAO.

raises the question of how catalysis is achieved in the absence of the lysine residue. For example, how does the protonation of the O2-site of the cofactor TPQ occur? Which residue takes over the function of the lysine? To address these questions a mechanism for the reductive half-reaction in the absence of the lysine has been investigated quantum chemically. Structural information for the present study is taken from the crystal structure for HPAO, which has been solved to 2.4 Å resolution.¹³ Unlike the crystal structure of PSAO,¹¹ the cofactor is already oriented as required for the catalysis in this structure (see Fig. 1). At the active site, the Cu atom is penta-coordinated in a distorted square-pyramidal geometry. It is bonded to the imidazole side chains of three histidines—His456, His458, and His624—and to two water molecules—one equatorial, and one axial. The substrate binding site is connected with copper through a hydrogen bonding network involving water molecules and an active site base Tyr305. In contrast to the earlier crystal structure, the C5 carbonyl of the cofactor and the substrate binding site are at the same side and the active site base (Asp319) is perfectly positioned to participate in the Schiff base formation. The Asp319, Tyr305, and Asn404 residues are conserved at the active site in all amine oxidases studied so far.²⁵ The above quantum chemically suggested mechanism coupled with the experimental information provide an excellent starting point for the further quantum chemical investigation of this enzyme.

Computational Details

The present calculations were performed using the GAUSSIAN-98²⁶ and Jaguar²⁷ programs. The calculations for the mechanism were performed in two steps. First, an optimization of the geom-

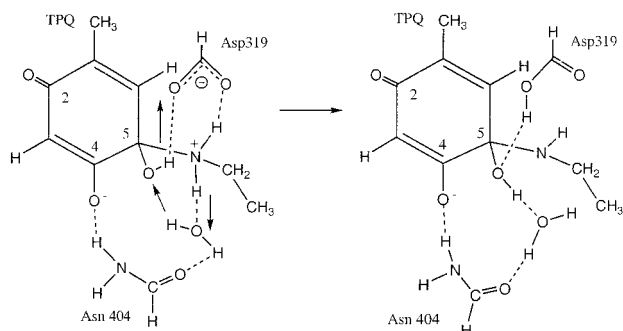


Figure 4. Suggested first part of the second step of the amine oxidation in HPAO.

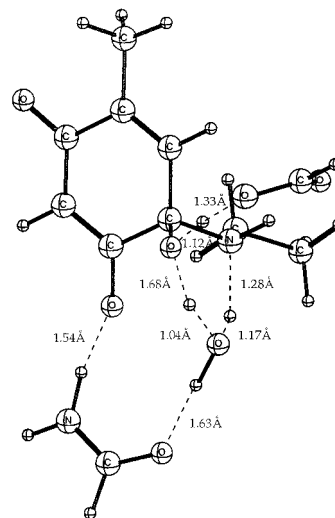


Figure 5. Optimized transition state for the first part of step 2.

etry was made using the B3LYP method²⁸ with the d95 basis set except for the first part of the third step of the mechanism (where copper is involved) where the lacvp basis set was used. Open-shell systems were treated using unrestricted B3LYP (UB3LYP). All degrees of freedom were optimized and the transition states obtained were confirmed to have only one imaginary frequency of the Hessian. In the second step, the B3LYP energy was evaluated for the optimized geometry using the large 6-311+G(2d,2p) basis set, which includes diffuse functions and two polarization functions on each atom. For the first part of the third step of the mechanism, the LACV3P** basis set of triple zeta, quality including one polarization function on each atom, was used together with an ECP²⁹ for the copper atom. Zero-point vibrational effects and thermal effects were added based on B3LYP calculations using the same basis set as for the geometry optimization. The dielectric effects from the surrounding environment were obtained using the CPCM polarizable conductor model (Cosmo),^{30,31} where the solvent cavity is formed as a surface of constant charge density of the solvated molecule. The default isodensity value of 0.0004 au is used. The radii of the solvent molecules were taken from the parameters for

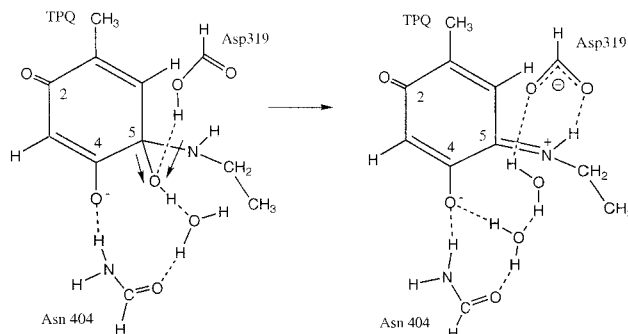


Figure 6. Suggested second part of the second step of the amine oxidation in HPAO.

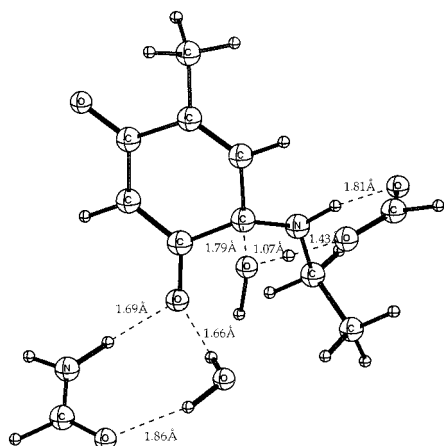


Figure 7. Optimized transition state for the second part of step 2.

water. The United Atom Topological Model³² was used to build the cavity around each heavy atom, and the radius of each atomic sphere was determined by multiplying the van der Waals radius by a scaling factor of 1.2. For the first part of the third step of the mechanism, the self-consistent reaction field method as implemented in Jaguar^{33,34} was used to evaluate the solvent corrections by employing the LACVP basis set. A probe radius of $R = 1.40$ Å corresponding to the water molecule was chosen. In both cases, the dielectric constant was set equal to 4, which corresponds to a dielectric constant of about 3 for the protein and 80 for the water medium surrounding the protein.³⁵ Because models with the same charge were used throughout the present study, the relative dielectric effects were found to be rather small and not very sensitive to the method used or to the value chosen for the dielectric constant. The relative energies discussed below are Gibbs free energies where all the effects described above are added. Normal errors of using B3LYP and different aspects of modeling enzyme active sites are described in recent reviews.^{36–38} To test the accuracy of the B3LYP method for the present systems, a comparison was made between the B3LYP and G2MS methods³⁹ in the previous DFT study of PSAO using the smallest possible models.¹⁹ A satisfactory deviation of only 2.0 kcal/mol between the G2MS and B3LYP levels was found.

Results and Discussion

An earlier DFT study of the first half-reaction (1) for PSAO,¹⁹ shown in Figure 2, prompted the present investigation of the

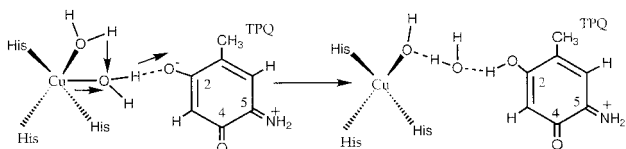


Figure 8. Suggested first part of the third step of the amine oxidation in HPAO.

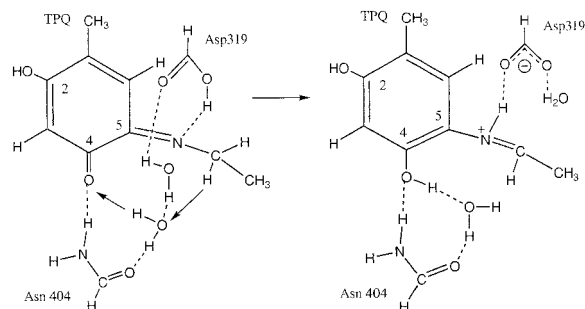


Figure 9. Suggested second part of the third step of the amine oxidation in HPAO.

reductive half-reaction of CAO in the absence of the active site lysine. Because the previous DFT study for PSAO and also experiments suggest that the copper complex is unlikely to play any role in the major part of the reaction,^{19,40} it could be left out of the model in most steps. The only exception is the first part of step 3, where the copper complex was included to protonate the cofactor TPQ. Because Asp319 is expected to play essentially the same role here as played by Asp300 in the earlier study for PSAO, it was included in the model. In the crystal structure of *H. polymorpha*,¹³ Asn404 is positioned only 4.30 Å away from the O4-site of TPQ, which makes it a likely candidate to participate in the mechanism. In HPAO, Asn404 and a water molecule together are expected to have the same role as played by Lys296 in PSAO,¹⁹ and were therefore included in some of the steps. The role of Asn404 was investigated in a few cases discussed below, by removing it from the model and using only a water molecule instead. The asparagine residue has also been suggested to be important for the initial positioning of the TPQ cofactor.⁴¹ In the case of PSAO, a neutral model was chosen for the first geometry optimization, but in the present study, in the absence of lysine, the system starts out negatively charged. A neutral form of the substrate and Asp319, and a negatively charged TPQ cofactor as suggested by experiments⁴² were chosen. It has to be stressed that this initial choice

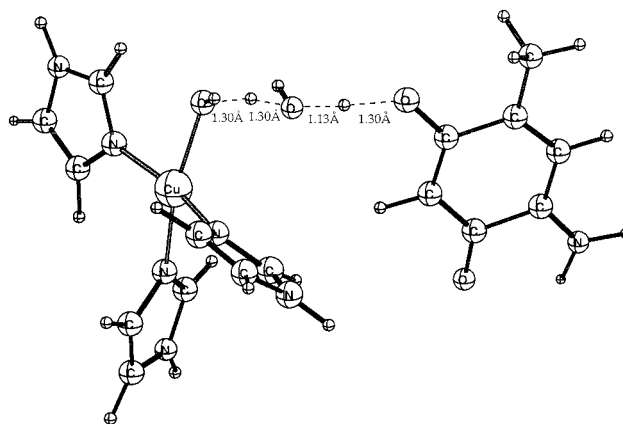


Figure 10. Optimized transition state for the first part of the third step of the amine oxidation in HPAO.

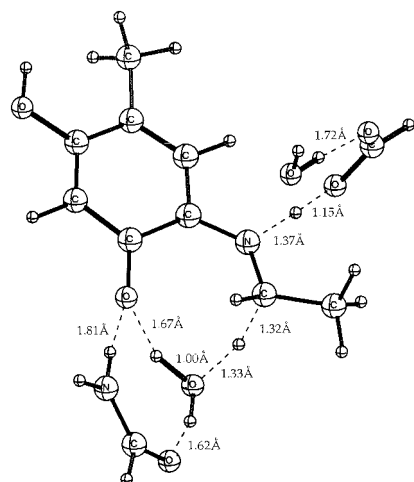


Figure 11. Optimized transition state for the second part of the third step of the amine oxidation in HPAO.

does not necessarily mean that the TPQ cofactor always remains negative. As discussed below, in some of the steps a neutral TPQ cofactor is also found. On the basis of earlier experience, a neutral Asp319 is modeled by a formic acid, while a neutral Asn404 is modeled by a formamide. The neutral substrate is modeled by an ethylamine.

Step 1. Substrate Attack on the C5 Site of TPQ

The first step of the suggested mechanism (see Fig. 3) involves an attack of the amine of the substrate on the C5 site of the cofactor TPQ with a simultaneous protonation of the O5 site by the neutral Asp319. This step is very similar to the first step in PSAO, the only difference being that the negatively charged form of TPQ was chosen here. The rest of the system, Asp319, and the substrate were chosen to be neutral, as they were in PSAO. A concerted attack on C5 and O5 is important to keep the barrier low. The step was found to have no barrier and is exothermic by 9.0 kcal/mol. The calculated entropy effect is +1.7 kcal/mol (included in the values), favoring the reactants and indicating that the product is more tightly bound than the reactant. On the other hand, due to the formation of the charged residues shown in the figure, the dielectric effects (also included in the values) favor the products by 1.5 kcal/mol. With the presence of lysine in PSAO, this step is perfectly thermoneutral, and crosses over a small barrier of 2.6 kcal/mol.

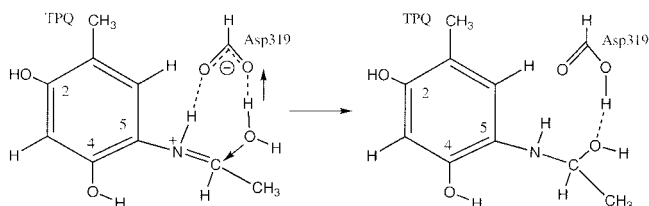


Figure 12. Suggested fourth step of the amine oxidation in HPAO.

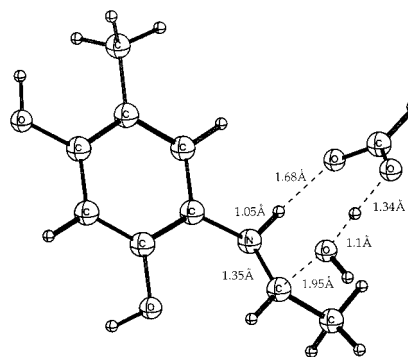


Figure 13. Optimized transition state for step 4.

Step 2. Formation of the Substrate Schiff Base

The suggested second step of the reaction mechanism describes the formation of the substrate Schiff base. This step is divided into two parts, shown in Figures 4 and 6. In PSAO (see Fig. 2), the formation of this base was suggested to proceed via a release of a water molecule, which is formed by a proton transfer from the amino group to the C5 hydroxyl group of TPQ via a solvent water molecule. In this step lysine was not suggested to be directly involved but only to stabilize the system by forming hydrogen bonds with the O4 and C5 hydroxyl group of TPQ. In the present study, the formation of the substrate Schiff base follows essentially the same mechanism, but with the difference that, here, Asn404 is hydrogen bonded to the O4 of TPQ and to a bridging water molecule. The substrate Schiff base has been observed experimentally in a crystal structure of the *Escherichia coli* enzyme with the 2-hydrazinopyridine inhibitor.²⁰ It has also been observed in model studies,^{42,43} by reductive trapping experiments^{44,45} and by resonance Raman²¹ spectroscopy. In the first part of this reaction step, a proton from the substrate amino group moves via a solvent water molecule over to the C-5 hydroxyl group. In turn, the hydroxyl proton is transferred to the unprotonated Asp319. In this proton transfer chain reaction, the substrate amino group becomes deprotonated and Asp319 protonated. This part has a barrier of 15.9 kcal/mol, and it is uphill by 8.4 kcal/mol. The transition state obtained is shown in Figure 5. In PSAO, this step has a 0.8 kcal/mol lower barrier and is 2.9 kcal/mol less endergonic.

After the first part of this step, the C—O bond distance to the C5 carbon and the O—H distance to Asp319 become the main reaction coordinates, and a water molecule is formed. The result-

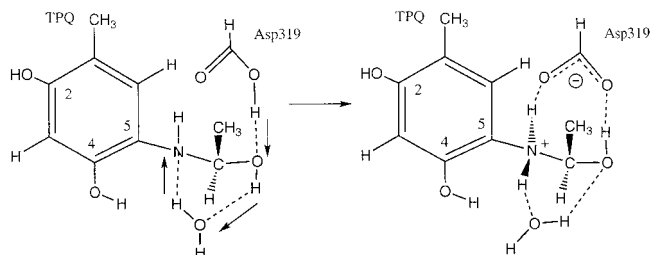


Figure 14. Suggested fifth step of the amine oxidation in HPAO.

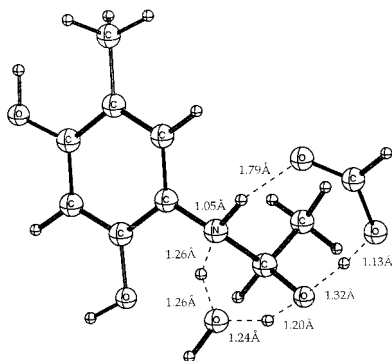


Figure 15. Optimized transition state for step 5.

ing transition state is shown in Figure 7. This part has a barrier of only 4.5 kcal/mol compared to the barrier in PSAO of 8.1 kcal/mol compared to the barrier in PSAO of 8.1 kcal/mol. Going from reactants to products in step 2 is exothermic by 14.4 kcal/mol. The calculated entropy effect is -2.7 kcal/mol (included in the values) favoring the product, and is due to the release of the water molecule. The overall exothermicity from the reactants to the products in step 2 is 5.9 kcal/mol, whereas in PSAO, it is only 2.5 kcal/mol. The calculated entropy effect contributes by -3.2 kcal/mol, and is mainly due to the release of the water molecule. In PSAO, with lysine present, this whole step has a 0.8 kcal/mol lower barrier and is 3.4 kcal/mol less exergonic. A calculated exothermicity of the second step agrees well with the inhibitor crystal structure of the enzyme, which shows that the doubly bonded substrate Schiff base is more stable than the singly bonded reactant of this step. This step was also investigated without including the Asn404 residue in the model. In the absence of Asn404, the enzyme follows a slightly different mechanism. In the first part of the mechanism, a proton from the substrate amino group is transferred to the O4-site of TPQ via a solvent water molecule. In the next step, with the help of the same bridging water molecule, this proton is transferred again to the C5 hydroxyl group and water is formed. In the absence of Asn404, the overall barrier for the formation of the substrate Schiff base is 3.9 kcal/mol higher.

Step 3. Formation of the Product Schiff Base

The suggested step 3, in which the C—H bond of the substrate is cleaved, is the most critical step of the entire mechanism. As shown in the suggested mechanism for PSAO (see Fig. 2), this step

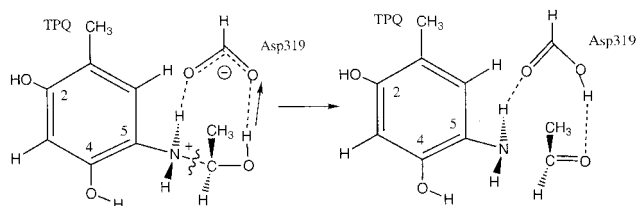


Figure 16. Suggested sixth step of the amine oxidation in HPAO.

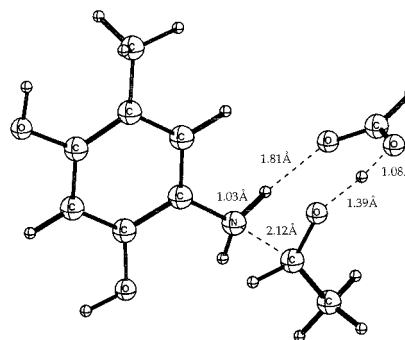


Figure 17. Optimized transition state for step 6.

leads to the formation of a second Schiff base, which is known as the product Schiff base. In the present study also, this step is divided into two parts, which are shown in Figures 8 and 9. The product Schiff base has recently been observed by resonance Raman spectroscopy of a mutant of yeast methylamine oxidase.^{23,24} It was shown in the previous study of PSAO, that to achieve the difficult task of C—H bond cleavage, the protonation of the O2-site of TPQ is necessary.¹⁹ In that study, a mechanism to accomplish O2 protonation was also suggested, in which a proton was transferred from Lys296 to the O2-site of TPQ through a hydrogen bonded chain including Tyr286 and two water molecules. The deprotonated lysine is then used in the actual C—H bond cleavage.

Without the lysine proton donor, the question arises how the O2-site of TPQ becomes protonated. It is not known with certainty that the copper complex is essential for this protonation, but its involvement has been suggested experimentally.^{46,47} In the X-ray structure, the axial water coordinated to copper is in the vicinity of the O2 site of TPQ,⁴⁸ which makes it a very likely candidate for participation in the protonation of O2. To investigate this possibility, the copper complex, including three histidines and two water molecules (axial and equatorial), is included in the model. In the first part of the third step (see Fig. 8), copper is initially penta-coordinated and TPQ is hydrogen bonded to the axial water molecule. During the course of the reaction, copper becomes tetra-coordinated by losing the axial water molecule, which moves over and bridges between the equatorial water and the O2-site of the TPQ cofactor. This point is actually in a local minimum. The formation of this intermediate is endergonic by 2.6 kcal/mol. This step has some similarities with the Cu—Zn superoxide dismutase (SOD), where Cu is also penta-coordinated and a water molecule is bonded at the axial position.⁴⁹ In SOD, this Cu-coordinated water molecule is easily replaced by small anionic ligands like cyanide and azide, which provides hydrogen bonding interactions to other water molecules within the active site.^{50,51} Once the tetra-coordinated intermediate structure is formed, a proton from the equatorial water molecule is transferred to the O2 position of the cofactor via the bridging water molecule. This proton transfer has a barrier of 2.8 kcal/mol. In the optimized transition state structure, shown in Figure 10, the water molecule is positioned between the copper metal center and the O2 position of the cofactor. Because this step follows a 2.6 kcal/mol endergonic step, the overall barrier for the proton transfer becomes 5.4 kcal/mol.

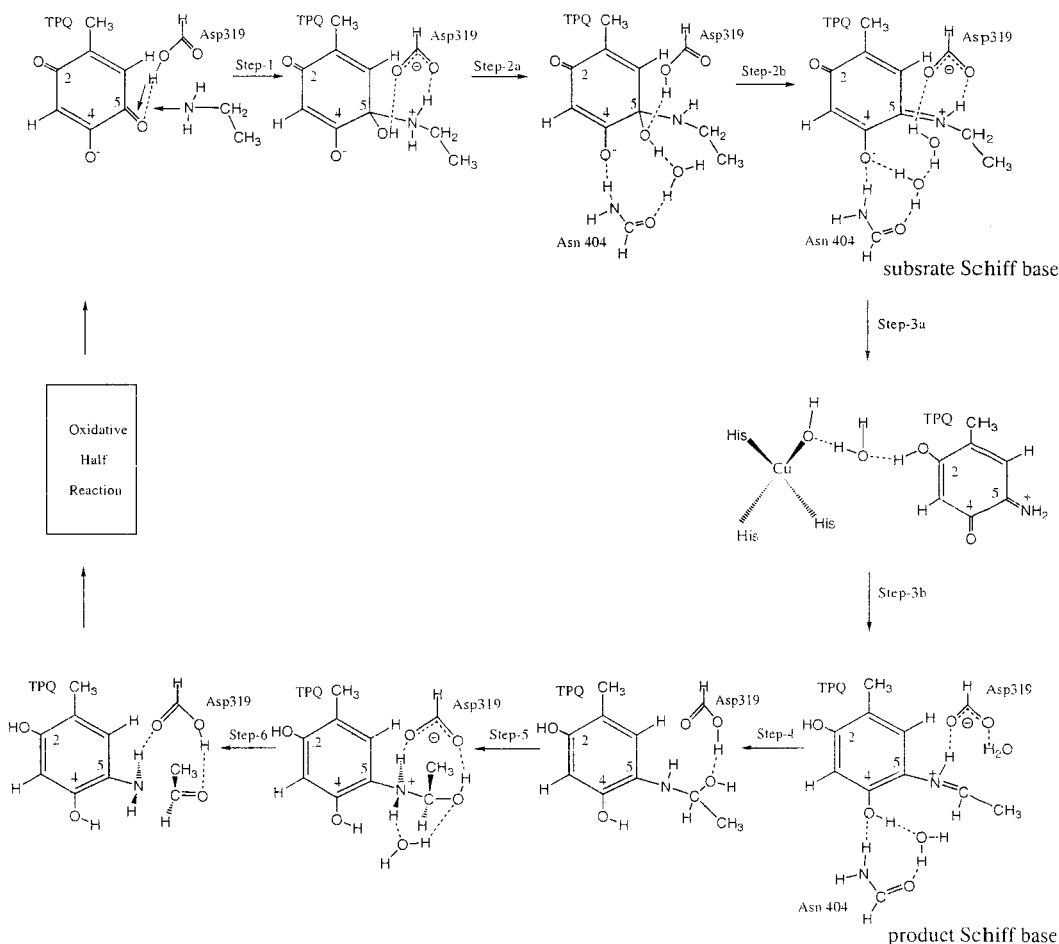


Figure 18. Suggested mechanism for the reductive half-reaction of copper amine oxidases where lysine is not present.

This step is slightly endergonic by 1.8 kcal/mol. In comparison, the suggested protonation of O₂ in PSAO passes a barrier of 10.1 kcal/mol and is endergonic by 8.1 kcal/mol. This result shows that the protonation of the O₂-site of TPQ by the copper complex in enzymes without lysine is more efficient than the suggested protonation by Lys296 in PSAO. Still, the calculations suggest that PSAO probably does not use this mechanism, because there is a big advantage if lysine is deprotonated for the next step of C—H activation. Overall, the calculated rate-limiting C—H activation is actually slightly lower with lysine present, see further below. Asp319 was not included in the model for the protonation of the O₄-site, but is required in the next step where it first takes a proton from the NH₂⁺ group at the C5 site of the TPQ cofactor and at the end gives it back. In this part, the critical C—H bond breaking takes place driven by a strong exothermicity of 16.7 kcal/mol. The main contribution to this driving force comes from the aromaticity of the TPQ ring, obtained in this step. The entropy effects decrease the exothermicity by 0.5 kcal/mol, and the dielectric effects give an increase by 0.4 kcal/mol. In PSAO, this part is even more exergonic by 28.5 kcal/mol. The transition state for this step is shown in Figure 11. At the end of this step Asp319 is unprotonated in agreement with some experimental suggestions.²³ During the

optimization, the water molecule which was formed in step 2, is hydrogen bonded to the second oxygen of the Asp319 carboxylate, swings around, and places itself close to the substrate C1 carbon. At this position it is in a perfect position for the next step.

The barrier for the C—H activation step is 17.1 kcal/mol. Because this part follows a step that is endergonic by 1.8 kcal/mol, see above, the overall barrier for the C—H bond cleavage becomes 18.9 kcal/mol. The barrier of 18.9 kcal/mol makes it the rate-limiting step of the presently suggested mechanism for the entire reductive half-reaction. This result is in agreement with rapid scanning kinetic data²² which suggest that the formation of the product Schiff base takes place in the rate-limiting step. For PSAO, the presence of lysine leads to a slightly lower barrier of 16.5 kcal/mol. Kinetic isotope effects have been calculated by replacing hydrogen by deuterium on the CH₂ group of the substrate. The calculated kinetic isotope effect of 4.6 is higher than the kinetic isotope effect of 3.9 for PSAO but lower than the experimental isotope effect of 8.5. Tunneling effects can be estimated using the simple Wigner formula⁵² and leads to an increase of the isotope effect to 5.8 in somewhat better agreement with experiment. To reach higher accuracy a more advanced dynamical treatment is necessary. Some more possibilities were explored for the

Table 1. Energies (kcal/mol) for the Optimized Structures of the Different Steps.

	E_{Bigbasis}	E_{DZ}	$E_{\Delta H}^a$	E_{Solv}^b	$E_{T\Delta S}$
Step-1					
0.0	0.0	0.0	0.0	0.0	0.0
-9.0	-12.2	-14.1	3.0	-1.5	1.7
Step-2a					
-9.0	0.0	0.0	0.0	0.0	0.0
6.9	18.8	13.5	-4.5	-0.4	2.0
-0.5	9.1	9.7	-1.7	1.5	-0.4
Step-2b					
-0.5	0.0	0.0	0.0	0.0	0.0
4.0	3.9	0.9	-0.3	-0.7	1.6
-14.9	-10.2	-4.7	0.3	-1.9	-2.7
Step-3a					
-14.9	0.0	0.0	0.0	0.0	0.0
-12.3	0.6	-2.2	-1.4	3.8	-0.5
-9.5	5.7	1.4	-2.9	4.9	-2.4
-13.1	-3.0	6.5	-2.5	5.2	2.0
Step-3b					
-13.1	0.0	0.0	0.0	0.0	0.0
4.0	20.3	15.4	-4.7	1.4	0.1
-29.8	-15.6	-25.4	-1.2	-0.4	0.5
Step-4					
-29.8	0.0	0.0	0.0	0.0	0.0
-17.6	8.8	4.1	-0.3	0.4	3.3
-25.1	-2.8	-3.4	1.4	2.1	4.0
Step-5					
-28.0	0.0	0.0	0.0	0.0	0.0
-16.0	15.7	6.8	-4.8	-0.8	1.9
-29.6	-0.4	-3.0	-0.7	-1.8	1.3
Step-6					
-29.6	0.0	0.0	0.0	0.0	0.0
-23.9	8.4	8.5	-1.4	-0.2	-1.1
-28.7	5.3	8.0	-0.5	0.6	-4.6

^aThe sum of zero-point and thermal enthalpy effects.^bCalculated with DZ basis set.

C—H bond-breaking step. Removing the asparagine raised the barrier by as much as 5.8 kcal/mol, showing that this residue is actually quite important for this step. Letting Asp319 take the role of Asn404 lowers the barrier by 0.2 kcal/mol, but this is not very likely because a large displacement of Asp310 is needed and it is very strongly hydrogen bonded to the nitrogen of the substrate. Removal of both Asn404 and the water molecule increases the barrier by 4.5 kcal/mol, showing that participation of these residues helps in the C—H bond breaking.

Step 4. Substrate C—OH Bond Formation

The suggested fourth step in the present study is exactly the same as the one for PSAO. In this step, (see Fig. 12) the C1 carbon of the substrate is attacked by the water molecule formed in step 2. After its formation, the water molecule is hydrogen-bonded to the Asp319, but in the course of step 3, it swings around 180 degrees (see above) and positions itself in the vicinity of the C1 of the substrate. In PSAO, the lysine does not participate in this step but

remains hydrogen bonded to the O4 hydroxyl group. The transition state for the formation of the C—O bond is shown in Figure 13. The calculated barrier is 12.2 kcal/mol, to which entropy effects contribute by +3.3 kcal/mol. This contribution comes mainly from the presence of a relatively free water molecule before the reaction with a large entropy. Dielectric effects raise the barrier by 0.4 kcal/mol. This step is endergonic by 4.7 kcal/mol, where entropy again contributes significantly by +4.0 kcal/mol. Solvent effects increase the endothermicity by 2.1 kcal/mol. The reason for the significant dielectric effects is a change of dipole moment from 6.4 to 2.1 D for the products. In PSAO, this step has very similar energetics, the barrier is 0.4 kcal/mol lower, and it is 1.6 kcal/mol less endergonic.

Step 5. Transfer of a Proton from Asp319 to the Substrate Nitrogen

The suggested fifth step is also very similar to the one in PSAO. In this step (see Fig. 14) a proton from the carboxylate of Asp319 is transferred to the substrate nitrogen in a concerted transfer over three hydrogen bonds. A water molecule is used to bridge the donor and acceptor sites. Because strong hydrogen bonds between Asp319 and the substrate hydroxyl group prevents Asp319 to swing around 180 degrees and deliver the proton directly to the substrate nitrogen, the present suggestion seems to be the best one. The optimized transition state is shown in Figure 15. As seen in this figure, the proton transfer is a strongly concerted process with several O—H and N—H distances in the range 1.1–1.3 Å. The computed barrier height is 12.0 kcal/mol, where zero-point vibrational (plus thermal enthalpy) effects have lowered the barrier significantly by 4.8 kcal/mol. The fifth reaction step is exergonic by 1.6 kcal/mol. In PSAO, this step has 1.4 kcal/mol lower barrier and it is 1.1 kcal/mol less exergonic.

Step 6. Formation of Product Aldehyde

The last step of the suggested mechanism (see Fig. 16) also has large similarities with the last step in PSAO. This step results in the release of the product aldehyde. The water molecule, which was added in the previous step, does not play any role in this step, and it was therefore removed from the model. To release the product aldehyde, the C—N bond of the substrate needs to be broken. The C—N bond breaking is achieved by a proton abstraction by Asp319. This is another critical function of Asp319 in the reductive half-reaction. The barrier for this step is 5.7 kcal/mol and the optimized transition state is shown in Figure 17. This step is slightly uphill by 0.9 kcal/mol. Entropy effects favor the product by 4.6 kcal/mol mainly due to the release of the product aldehyde. In PSAO, it was not possible to find a transition state for this step due to a very small barrier for the backward reaction. It was found to be 5.0 kcal/mol more endergonic. This step was expected to be exergonic, and the endothermicity is therefore rather surprising. The reason behind this might be that there is a very strong hydrogen bond, with a bond distance of 1.54 Å between Asp319 and the product aldehyde. It is suggested by experiments that after the release of the product, Asp319 becomes deprotonated.⁴⁸ In that scenario, this hydrogen bond will be replaced by hydrogen bonds to other residues, and aldehyde would become much more free,

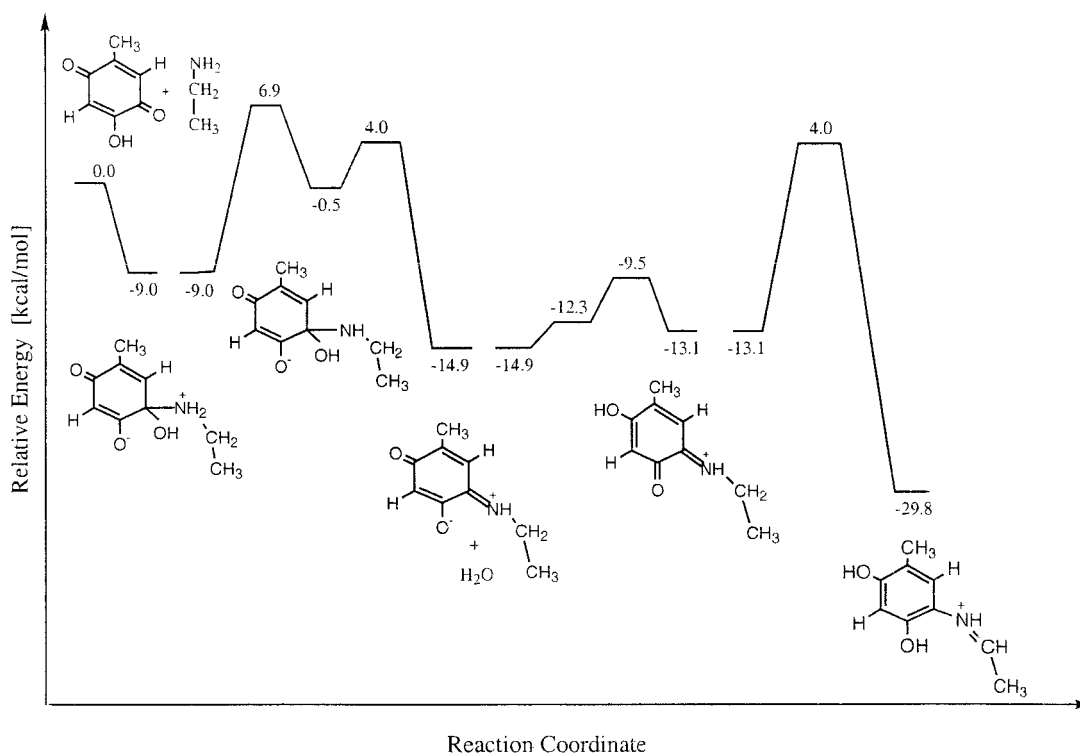


Figure 19. Energy diagram for the first three steps of the reductive half reaction of HPAO.

and a gain of entropy would probably make this step exothermic. Because this reaction would require a significantly larger model than the one presently used, this part of the final step of the reductive half-reaction was not studied further. At the end of the reductive half-reaction the cofactor is in its reduced aminoquinol form. In the oxidative half-reaction it will be oxidized back to its original TPQ form.

Summary

The reductive half-reaction for those CAOs that do not have an active site lysine has been studied using similar kinds of computational methods and models as used previously for the reductive half-reaction of PSAO,¹⁹ the oxidative half-reaction of CAO⁵³ and for different substrate reactions of other enzymes like RNR^{54,55} and PFL.⁵⁶ The present study was prompted by the need to address the role of lysine implied to be important in the previous quantum chemical study of PSAO,¹⁹ but which is not present in other CAOs. All the steps are compared with the mechanism suggested for PSAO (see Fig. 2). The available structural and spectroscopic information provided by experiments was also fully utilized in the present quantum chemical study. The overall mechanism suggested in the present study is shown in Figure 18. The detailed energy contributions of each step are given in Table 1. Like PSAO, the energy diagrams are divided into six steps (see Figs. 19 and 20). Steps 2 and 3 are further subdivided into two steps each. The energy diagrams were constructed by imposing the constraint that

the reactant of each step should have the same energy as the product of the previous step. Step 5 is the only exception to this rule, and the product of step 5 is placed at a calculated energy of 0.2 kcal/mol higher than the reactant of step 4. The reason behind this minor adjustment is that in step 5 an extra water molecule was added in the model, whereas in the fourth and sixth step the same size of models were used. The reactant of the sixth step was calculated to be 0.2 kcal/mol higher than the reactant of the fourth step using the same model. It is known from experiments that the product of step 5 should be lower than the reactant of step 4, and placing the reactant of step 5 at the same energy as the product of step 4 would create a larger disagreement with experiments. A similar kind of minor adjustment was made for PSAO, where the product of step 5 was placed 0.4 kcal/mol lower than the reactant of step 4. By taking the accuracy of the present methods into account, the agreement with experiments is quite satisfactory overall.

In the first step of the presently suggested mechanism an exergonic addition of the amine substrate to the C5 carbon of TPQ takes place with a simultaneous protonation of O5 by Asp319. This step has no barrier, and is exergonic by 9.0 kcal/mol. In the second step, a protonation of the O5 hydroxyl group of TPQ leads to the formation of a water molecule. In the first part of this step, a proton from the N1 substrate group is transferred via a water molecule to the O5 hydroxyl group, which in turn, passes it on to Asp319. This part has a barrier of 15.9 kcal/mol and is endergonic by 8.4 kcal/mol. In the second part, Asp319 donates this proton back and a water molecule is formed. The second part has a barrier of 4.5

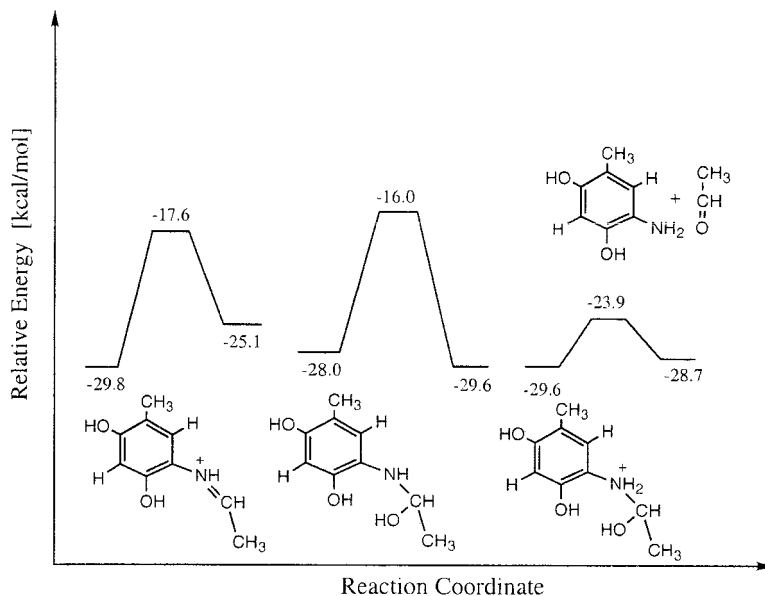


Figure 20. Energy diagram for the last three steps of the reductive half reaction of HPAO.

kcal/mol, and is exergonic by 14.4 kcal/mol. This step results in the formation of the substrate Schiff base, which has been observed experimentally in a crystal structure with an inhibitor²⁰ and by resonance Raman spectroscopy.²¹ An overall exothermicity in this step is in agreement with experiments that observe only the substrate Schiff base but not the singly bonded reactant of this step. The third step describes the formation of the product Schiff base, and is experimentally suggested to be the rate-limiting step of the entire reductive half-reaction.²² This step is also subdivided into two parts. In the first part, as suggested by experiments, the TPQ cofactor is protonated at the O2 position by the copper complex.⁴⁶ This part has an overall barrier of 5.4 kcal/mol, and is endergonic by 1.8 kcal/mol. In the second part of this step, a proton from the C1 site of the substrate is transferred over to the O4-site of TPQ. This proton transfer is assisted by Asn404 and a water molecule. As suggested by experiments, Asp319 does not participate in this step and remains unprotonated.²³ The second part has a barrier of 17.1 kcal/mol. Because this part follows a step that is endergonic by 1.8 kcal/mol, the overall barrier for this step becomes 18.9 kcal/mol. The formation of the product Schiff base is highly exergonic by 16.7 kcal/mol. It has been observed experimentally by resonance Raman spectroscopy for an E406N mutant of yeast methylamine oxidase.^{23,24} Step 4 has a barrier of 12.2 kcal/mol, and is endergonic by 4.7 kcal/mol. In step 5, Asp319 gets deprotonated by transferring its proton to the substrate through an external water molecule. This step is exergonic by 1.6 kcal/mol, and crosses over a barrier of 12.0 kcal/mol. Finally, in the last step, the C—N bond is broken and the product aldehyde is formed. This step has a barrier of 5.7 kcal/mol, and is slightly endergonic by 0.9 kcal/mol. The present mechanism suggested by the model calculations (see Figs. 19 and Fig. 20), is in good agreement with most of the available experimental information. Detailed energetics of each reaction step has provided a deeper understanding of the catalytical function of this interesting enzyme.

References

1. Parrott, S.; Jones, S.; Cooper, R. A. *J Gen Microbiol* 1987, 133, 347.
2. Cooper, R. A.; Knowles, P. F.; Brown, D. E.; McGuirl, M. A.; Dooley, D. M. *Biochem J* 1992, 288, 337.
3. Hacisalihoglu, A.; Jongejan, J. A.; Duine, J. A. *Microbiology* 1997, 143, 505.
4. McIntire, W. S.; Hartmann, C. In *Principles and Application of Quinoproteins*; Davidson, V. L., Ed.; Marcel Dekker: New York, 1993; p 97.
5. Morgan, D. L. M. *Methods Mol Biol* 1998, 79, 3.
6. Ha, H. C.; Woster, J. D.; Yager, J. D.; Casero, R. A. *Proc Natl Acad Sci USA* 1997, 94, 11557.
7. Knowles, P. F.; Dooley, D. M. In *Metal Ions in Biological Systems*; Sigel, H.; Sigel, A., Ed.; Marcel Dekker: New York, 1994; 30, 361.
8. McIntire, W. S. *FASEB J* 1994, 8, 513.
9. Tanizawa, K. *J Biochem* 1995, 118, 671.
10. Parsons, M. R.; Convery, M. A.; Wilmot, C. M.; Yadav, K. D. S.; Blakeley, V.; Corner, A. S.; Phillips, S. E. V.; McPherson, M. J.; Knowles, P. F. *Structure* 1995, 3, 1171.
11. Kumar, V.; Dooley, D. M.; Freeman, C. H.; Guss, J. M.; Harvy, I.; McGuirl, M. A.; Wilce, M. C. J.; Zubak, V. M. *Structure* 1996, 4, 943.
12. Wilce, M. C. J.; Dooley, D. M.; Freeman, C. H.; Guss, J. M.; Matsunami, H.; McIntire, W. S.; Ruggiero, C. E.; Tanizawa, K.; Yamaguchi, H. *Biochemistry* 1997, 36, 16116.
13. Li, R.; Klinman, J. P.; Mathews, F. S. *Structure* 1998, 6, 293.
14. Chen, Z.; Schwartz, B.; Williams, N. K.; Li, R.; Klinman, J. P.; Mathews, F. S. *Biochemistry* 2000, 39, 9709.
15. Cai, D.; Klinman, J. P. *J Biol Chem* 1994, 269, 32039.
16. Matsuzaki, R.; Fukui, T.; Sato, H.; Ozaki, Y.; Tanizawa, K. *FEBS Lett* 1994, 351, 360.
17. Knowles, P. F.; Yadav, D. S.; *Copper Proteins and Copper Enzymes*; Lontie, R., Ed.; CRL Press: Boca Raton, FL, 1984; p 103.
18. Palcic, M. M.; Klinman, J. P. *Biochemistry* 1983, 22, 5957.
19. Prabhakar, R.; Siegbahn, P. E. M. *J Phys Chem B*, 2001, 105, 4400.
20. Wilmot, C. M.; Murray, J. M.; Gordon, A.; Parsons, M. R.; Convery,

- M. A.; Blakeley, V.; Corner, A. S.; Palcic, M. M.; Knowles, P. F.; McPherson, M. J.; Phillips, S. E. V. *Biochemistry* 1997, 36, 1608.
21. Brown, D. E.; McGuirl, M. A.; Dooley, D. M.; Janes, S. M.; Mu, D.; Klinman, J. P. *J Biol Chem* 1991, 266, 4049.
 22. Hartmann, C.; Brzovic, P.; Klinman, J. P. *Biochemistry* 1993, 32, 2234.
 23. Cai, D.; Dove, J.; Nakamura, N.; Sanders-Loehr, J.; Klinman, J. P. *Biochemistry* 1997, 36, 11472.
 24. Klinman, J. P. *J Biol Chem* 1996, 271, 27189.
 25. Tipping, A. J.; McPherson, M. J. *J Biol Chem* 1995, 270, 16939.
 26. Frisch, M. J.; Trucks, G. W.; Schlegel, H. B.; Scuseria, G. E.; Robb, M. A.; Cheeseman, J. R.; Zakrzewski, V. G.; Montgomery, J. A.; Stratmann, R. E.; Burant, J. C.; Dapprich, S.; Millam, J. M.; Daniels, A. D.; Kudin, K. N.; Strain, M. C.; Farkas, O.; Tomasi, J.; Barone, V.; Cossi, M.; Cammi, R.; Mennucci, B.; Pomelli, C.; Adamo, C.; Clifford, S.; Ochterski, J.; Petersson, G. A.; Ayala, P. Y.; Cui, Q.; Morokuma, K.; Malick, D. K.; Rabuck, A. D.; Raghavachari, K.; Foresman, J. B.; Cioslowski, J.; Ortiz, J. V.; Stefanov, B. B.; Liu, G.; Liashenko, A.; Piskorz, P.; Komaromi, I.; Gomperts, R.; Martin, R. L.; Fox, D. J.; Keith, T.; Al-Laham, M. A.; Peng, C. Y.; Nanayakkara, A.; Gonzalez, C.; Challacombe, M.; Gill, P. M. W.; Johnson, B. G.; Chen, W.; Wong, M. W.; Andres, J. L.; Head-Gordon, M.; Replogle, E. S.; Pople, J. A. *Gaussian, Inc.; Pittsburgh, PA*, 1998.
 27. JAGUAR 4.1: Schrödinger, Inc.; Portland, Oregon, 2000. See: Vacek, G.; Perry, J. K.; Langlois, J.-M. *Chem Phys Lett* 1999, 310, 189.
 28. Becke, A. D. *Phys Rev* 1988, A38, 3098; Becke, A. D. *J Chem Phys* 1993, 98, 1372; Becke, A. D. *J Chem Phys* 1993, 98, 5648.
 29. Hay, P. J.; Wadt, W. R. *J Chem Phys* 1985, 82, 299.
 30. Barone, V. M.; Cossi, M. *J Phys Chem A* 1998, 102, 1995.
 31. Klamt, A.; Schuurmann, G. *J Chem Soc Perkin Trans 2* 1993, 5, 799.
 32. Barone, V. M.; Cossi, M.; Tomasi, J. *J Chem Phys* 1997, 107, 3210.
 33. Tannor, D. J.; Marten, B.; Murphy, R.; Friesner, R. A.; Sitkoff, D.; Nicholls, A.; Ringnalda, M.; Goddard, W. A., III; Honig, B. *J Am Chem Soc* 1994, 116, 11875.
 34. Marten, B.; Kim, K.; Cortis, C.; Friesner, R. A.; Murphy, R. B.; Ringnalda, M.; Sitkoff, D.; Honig, B. *J Phys Chem* 1996, 100, 11775.
 35. Blomberg, M. R. A.; Siegbahn, P. E. M.; Babcock, G. T. *J Am Chem Soc* 1998, 120, 8812.
 36. Siegbahn, P. E. M.; Blomberg, M. R. A. *Annu Rev Phys Chem* 1999, 50, 221.
 37. Siegbahn, P. E. M.; Blomberg, M. R. A. *Chem Rev* 2000, 100, 421.
 38. Siegbahn, P. E. M.; Blomberg, M. R. A. *J Phys Chem* 2001, 105, 9375.
 39. Froese, D. J.; Humbel, S.; Svensson, M.; Morokuma, K. *J Phys Chem* 1997, 101, 227.
 40. Medda, R.; Padiglia, A.; Pedersen, J. Z.; Rotilio, G.; Agró, A. F.; Floris, G. *Biochemistry* 1995, 34, 16375.
 41. Schwartz, B.; Edward, L. G.; Sanders-Loehr, J.; Klinman, J. P. *Biochemistry* 1998, 37, 16591.
 42. Mure, M.; Klinman, J. P. *J Am Chem Soc* 1993, 115, 7117.
 43. Mure, M.; Klinman, J. P. *J Am Chem Soc* 1995, 117, 8707.
 44. Hartmann, C.; Klinman, J. P. *J Biol Chem* 1987, 262, 962.
 45. Hartmann, C.; Klinman, J. P. *FEBS Lett* 1990, 261, 441.
 46. Klinman, J. P. *Chem Rev* 1996, 96, 2541.
 47. Mure, M.; Mills, M. A.; Klinman, J. P. *Biochemistry* 2002, 41, 9269.
 48. Wilmot, C. M.; Hajdu, J.; McPherson, M. J.; Knowles, P. F.; Phillips, S. E. V. *Science* 1999, 286, 1724.
 49. Hart, P. J.; Balbirnie, M. M.; Ogihara, N. L.; Nersissian, A. M.; Weiss, J. S.; Valentine, J. S.; Eisenberg, D. *Biochemistry* 1999, 38, 2167.
 50. Djinovic, K. C.; Battistoni, A.; Carri, M. T.; Polticelli, F.; Desideri, A.; Rotilio, G.; Coda, A.; Bolognesi, M. *FEBS Lett* 1994, 349, 93.
 51. Djinovic, K.; Polticelli, F.; Desideri, A.; Rotilio, G.; Wilson, K.; Bolognesi, M. *J Mol Biol* 1994, 240, 179.
 52. Wigner, E. P. *Phys Chem Abstr B1932*, 19, 203.
 53. Prabhakar, R.; Siegbahn, P. E. M. *J Phys Chem B*, in press.
 54. Siegbahn, P. E. M. *J Am Chem Soc* 1998, 120, 8417.
 55. Himo, F.; Siegbahn, P. E. M. *J Phys Chem B* 2000, 104, 7502.
 56. Himo, F.; Eriksson, L. A. *J Am Chem Soc* 1998, 120, 11449.